Heat Transport at Solid-Liquid Interfaces between Face-Centered Cubic Lattice and Liquid Alkanes

Abdul Rafeq Saleman[1,*], Fudhail Abdul Munir[1], Mohd Rody Mohammad Zin[1], Mohd Shukri Yob[1], Gota Kikugawa[2], Taku Ohara[2]

[1] Centre of Advanced Research on Energy, Fakulti Kejuruteraan Mekanikal, Universiti Teknikal Malaysia Melaka, Hang Tuah Jaya, 76100 Durian Tunggal, Melaka, Malaysia
[2] Institute of Fluid Science, Tohoku University, 2-1-1 Katahira Aoba-ku, Sendai 980-8577, Japan

ARTICLE INFO	ABSTRACT
	Solid-liquid (S-L) interfaces is widely used in lubrication and coating systems, in which the heat transport is the main problem for the system. In the recent years, lubrication and coating systems have been investigated up to the molecular scale to solve the problem of heat transport due to wear and friction. In molecular scale, the characteristics of heat transport are different from the conventional one. Therefore, the purpose of this study is to specifically investigate the characteristics of heat transport in the molecular scale at the S-L interfaces. The prime concern in this numerical investigation is the surface structure of solid and the type of liquid molecules. The characteristics of heat transport at the S-L interfaces are evaluated based on the temperature jump (TJ) and thermal boundary resistance (TBR) at the interfaces. It is found that the different TJs and TBRs can be observed for variation of the surface structures and the length of liquid molecules. The obtained results show that the surface structures and length of liquid molecules significantly affect the characteristics of heat transport at S-L interfaces.

1. Introduction

Solid-liquid (S-L) interfaces have been widely utilized for tribology applications that are related to lubrication and coating systems [1–5]. Examples of these applications are characterization of thermal interface materials, production of magnetic hard disc and journal bearing design. In the past, there are abundant of literatures that focus on the lubrication and coating systems to address the problem of wear and friction at the contacting surfaces, such as self-lubrication [6,7], hard-wear resistance coating [2,8], and nano-lubricant [3]. However, in recent years, due to the development of nanotechnology, most of the lubrication and coating systems are investigated at the molecular-scale. Based on the previous studies [9–16], it was reported that the systems that are in the

---

* Corresponding author.
E-mail address: rafeq@utem.edu.my (Abdul Rafeq Saleman)

molecular-scale have anomalous characteristics that could not be easily determined or predicted based on the conventional macroscopic concepts. In order to address such problems, molecular dynamics (MD) simulation can be utilized as the alternative tool to reproduce the molecular-scale phenomena for details analysis.

The system that are in molecular-scale especially for lubrication and coating systems, often needs to deal with heat generation and dissipation at interfaces. This heat generation can lead to failure if the heat dissipation technique is not adequately controlled in the system. In the lubrication and coating systems, the heat dissipation at the S-L interfaces can be properly explained by understanding the characteristics of heat transport at interfaces. As such, these characteristics of heat transport at S-L interfaces are critical in order to optimize the performance of a system.

In the past, there are a number of investigations that focus on the characteristics of heat transport at S-L interfaces such as the influences of molecular interactions between solid and liquid [14,17–21] and surface roughness [22,23]. However, to this date, there is very limited signifcant study on the effect of surface structure of solid walls and the types of liquid molecules on the heat transport characteristics. Hence, this paper presents the characteristics of heat transport at S-L interfaces with the focus on the surface structure of solid and types of liquid molecules.

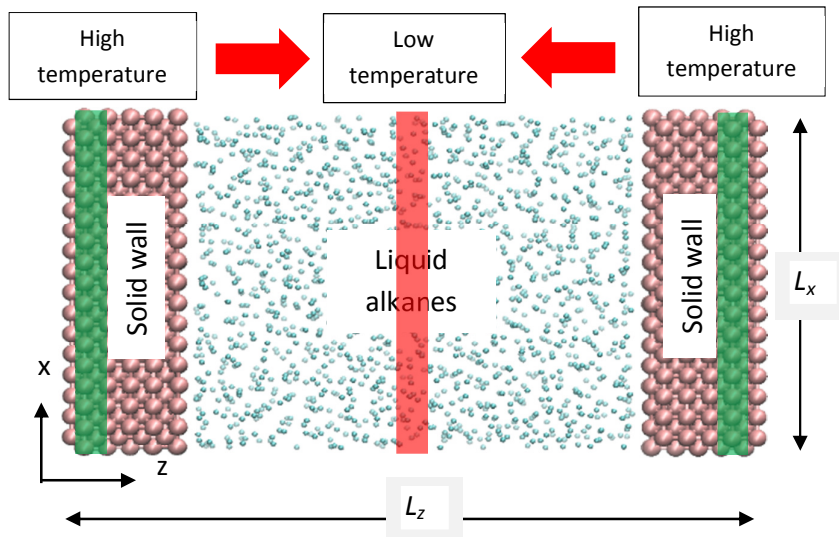## 2. Simulation Details
2.1 Simulation System

Fig. 1. Simulation system of the liquid sandwiched between two parallel solid walls
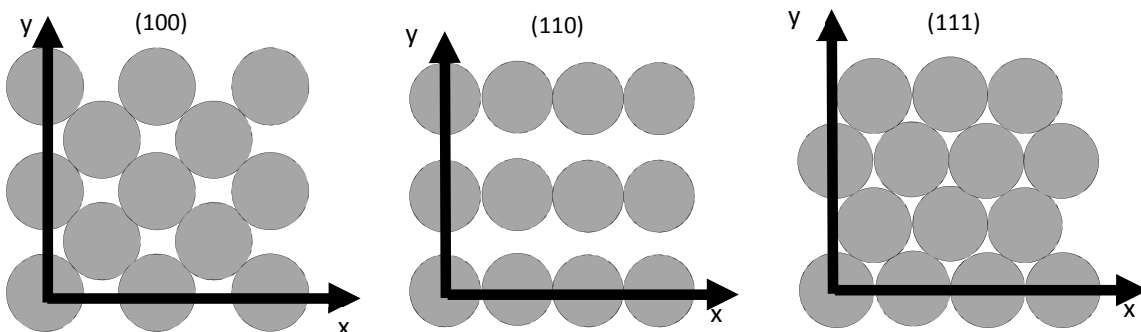

Fig. 2. Surface structure of (100), (110) and (111) lattices

Figure 1 shows the simulation system, which consists of liquid that is sandwiched between two parallel solid walls. The solid wall is a face-centered cubic (FCC) lattice with the surfaces of (100), (110) and (111) in contact with the liquid. The surface structure of the (100), (110) and (111) lattices is shown in Fig. 2. An identical surface is utilized on both (left and right) sides of the simulation system. The contact surfaces of solid and liquid on the left and right sides of the simulation system are referred here as S-L interfaces

2.2 Potential Functions

The liquid consists of liquid alkanes that namely are methane (CH_4) and butane (C_4H_{10}). In this study the liquid alkanes is modelled using united atom (UA) model. In the UA model, the hydrogen atom is grouped in a single interaction site located at the carbon atom that represented as pseudoatom. The pseudoatom connected to another pseudoatom to represent linear alkane molecules [24–26]. The UA NERD potentials is utilized in the present system to modelled C_4H_{10} liquid. The UA NERD potentials consists of bond bending, bond stretching, torsion and non-bonded interaction where the details of the potential functions and parameters are found elsewhere [26–28]. For the CH_4 liquid, it was modelled by Transferable Potential for Phase Equilibria (TraPPE) force field, where the UA was utilized to model the CH_4 molecules as a pseudoatom. The parameters for the interaction between each pseudoatom is described by using the Lennard Jones 12-6 (LJ) potentials [29]. The LJ potential is given as follows

$$U^{LJ}(r_{ij}) = 4\varepsilon_{ij}\left[\left(\frac{\sigma_{ij}}{r_{ij}}\right)^{12} - \left(\frac{\sigma_{ij}}{r_{ij}}\right)^{6}\right] \tag{1}$$

The r_{ij} is the distance between atoms i and j. The energy parameters are ε_{ij} = 2.0433 × 10^{-21} and σ_{ij} = 3.73 Å. The solid walls is describe by Morse potentials, the same potentials have been utilized in ref [30]. The Morse potentials is given as follow

$$\Phi(r_{ij}) = D[e^{-2\alpha(r_{ij}-r_o)} - 2e^{-\alpha(r_{ij}-r_o)}] \tag{2}$$

The D = 7.6148 × 10^{-20} J, r_0 = 3.0242 Å and α = 1.5830 Å^{-1} [31]. r_{ij} is the distance between atoms i and j. The interaction between solid atom and liquid molecules was modelled by the LJ potentials and the parameters for the interaction were calculated based on the Lorentz-Bertholet (LB) combining rules. The LB combining is given as follow

$$\varepsilon_{sl} = \sqrt{\varepsilon_{ss}\varepsilon_{ll}}, \text{ and } \sigma_{sl} = \frac{\sigma_{ss} + \sigma_{ll}}{2}. \tag{3}$$

The s and l belong to solid and liquid respectively. The parameters of ε and σ for solid atom is given as 2.7109 × 10^{-22} J and 3.70 Å, respectively [32]. The interaction parameters were truncated beyond the cut-off radius of 12.0 Å. The size of the simulation systems were approximately 40 × 40 × 120 Å for the L_x, L_y and L_z, respectively. Periodic boundary condition was used on the x- and y-directions of the simulation system. The outermost layer of solid atoms was set to be fixed on its position as to ensure that the system is not fluctuating or drifting during simulation.

2.3 Simulation method

The reversible Reference System Propagator Algorithm (r-RESPA) method with multiple time step was utilized for the time integration. One femto second (fs) and 0.2 fs time integration was utilized for intermolecular motions and intramolecular motions respectively.

Initially the temperature of the simulations system was raised to the targeted temperature, at the 0.7 of the critical temperature (T_C) for the liquid using velocity scaling method. Then, the simulation system was equilibrated for 1 to 4 million time steps until a uniform temperature is acquired at the targeted temperature. After that, by using velocity scaling method, a high temperature was applied to two parallel solid walls and the low temperature was applied at the center of the liquid as shown in Fig. 1. The heat flux applied across the simulation system is approximately 200 MW/m^2 regardless the types of liquid alkanes and crystal planes. The simulation system was then run for 3 to 5 million time steps until steady state is acquire. After steady state is acquired, then the data acquisition step is run for 10 to 20 million time steps. The variation in the time step depend on the size of the liquid molecules, where longer molecular length of liquid required more time step to have the obtained data to be converged.

The thermal conductivities of present simulation system have been validated by the author's previous study [26]. The deviation between the experimental data and simulated one was approximately 20% for CH_4 liquid and 10% for C_4H_{10} liquid.

3. Results and Discussions
3.1 Temperature Distributions

In order to calculate the temperature distributions of the simulation system, it is first divided into a number of slabs. The definition of the slabs to calculated the temperature distributions is found elsewhere [27,33].

In the present simulation system, the temperature is calculated from the random velocity of each molecule. In this study the temperature distributions is divided into *x*-, *y*- and *z*-components since the random velocity of molecules consisted of *x*-, *y*- and *z*-directions. Figure 3 shows the temperature distributions in *x*-, *y*- and *z*-components for liquid CH_4 facing (110) lattice. The *x*-, *y*- and *z*- components of temperature is refer here as *Tx*, *Ty* and *Tz*, respectively. The similar profile of temperature distributions is observed for all cases of FCC lattices and liquid C_4H_{10}. It is found that near the S-L interfaces the distributions of thermal energy is different between the *Tx*, *Ty* and *Tz*. This can be considered as the nonequilibrium thermal energy which was also observed in previous study for shearing system [27]. This indicate that different component will generate different thermal energy transfer across the S-L interfaces.

In order to further understand the characteristics of thermal energy transfer across the S-L interfaces the temperature jump at the S-L interfaces is measured. The same evaluation of temperature jump as in ref [27] was utilized in the present study. Table 1 tabulated the value of temperature jump for CH_4 liquid and C_4H_{10} liquid in contact with (100), (110) and (111) lattices.

It is found that small temperature jump is observed for *Tz* regardless of the types of FCC lattices and types of liquid alkanes. For the cases of (100) and (111) crystal planes the value of *Tx* and *Ty* is almost similar, and *Tz* is the smallest among the components of temperature. However, for the case of (110) crystal plane the *Tx*, *Ty* and *Tz* is in the decreasing order, where *Tx* is the highest follow by *Ty* and the smallest is *Tz*. Based on temperature jump and surface structure of FCC lattices shown in Fig. 2, it is understood that different surface structure will generate different characteristics of temperature jump. It is found that the temperature jump for C_4H_{10} is slightly higher than CH_4 liquid,

this indicate the different size of liquid molecules will generate different thermal energy transfer which was also observed in previous study [26].
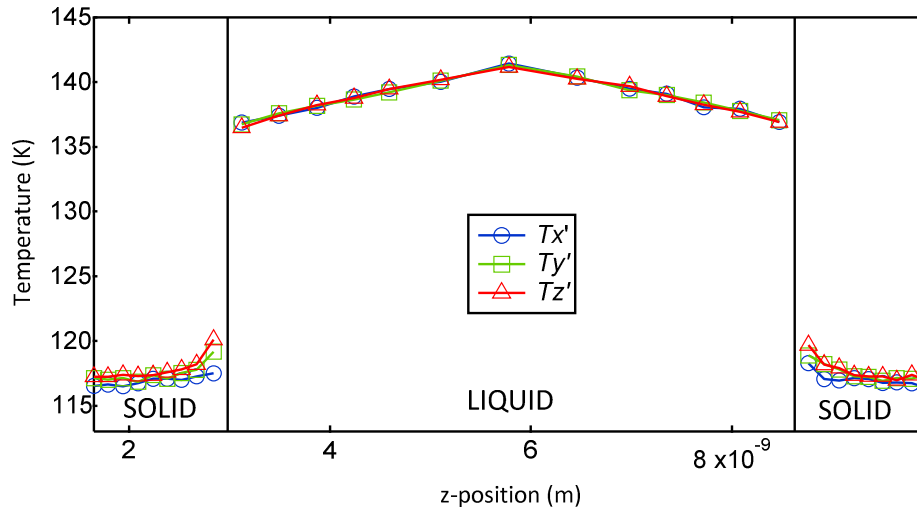

Fig. 3. Temperature distribution of Liquid CH_4 confined between the two parallel solid walls

Table 1
The temperature jump in Tx, Ty and Tz for CH_4 liquid and C_4H_{10} liquid

Crystal plane	CH_4 (Methane)				C_4H_{10} (Butane)			
	Temperature Jump (K)				Temperature Jump (K)			
	average	Tx	Ty	Tz	average	Tx	Ty	Tz
100	22.9	25.2	25.1	18.5	23.0	23.8	23.8	21.4
110	17.2	18.5	17.2	16.0	22.1	22.9	21.8	21.7
111	19.5	21.2	20.9	16.3	21.0	21.3	21.6	20.0

3.2 Thermal Boundary Resistance

Thermal boundary resistance (TBR) is the measurement of thermal energy resistance at the S-L interfaces. It is given as follows:

$$TBR = \frac{\Delta T}{J} \tag{4}$$

The ΔT represent the temperature jump and J is the heat flux applied throughout the simulation system. Since the temperature is divided in three components, the TBR is also divided into three x-, y- and z-components. The TBR in each component is calculated as follow; the average temperature jump is divided by the amount of heat flux measure in each x-, y- and z-components.

Table 2 shows the TBR for CH_4 liquid and C_4H_{10} liquid facing the (100), (110) and (111) lattices. Based on the value of TBR it is found that the TBR is in the order of (110), (111) and (100) lattices start from the lowest to the highest, regardless the types of liquid alkanes. In general, although the TBR in each component is not directly calculated from the components of temperature jump, the same trends is observed in the temperature jump of the Tx, Ty and Tz for the cases of (100), (110) and (111) lattices. Based on the observation, it suggests that the TBR is correlated with

temperature jump. For the cases of (100) and (111) lattices, the *x*- and *y*-components of TBR is larger than *z*-component, for both types of liquid alkanes. This indicate that z-component is the main contributor to the heat transport at the S-L interfaces and x, and y-components of TBR contribute less to the heat transport at the interfaces. It is found that different characteristics is observed for y-component of TBR for the case of (110) lattice, where the TBR is the lowest as compared to (100) and (111) lattice, regardless the types of liquid molecules. This indicate that y-component for the case of (110) lattice has larger contribution of heat transport at the S-L interfaces as compared to (100) and (111) lattice. As shown in Fig. 2, there is lattice corrugation along the x-axis of (110) lattice. The lattice corrugation enhances the heat transport at the S-L interfaces thus the heat transport from y-component is increased as observed in the y-component of TBR shown in table 2.

It is observed table 2 that the total value of TBR is larger for C_4H_{10} liquid as compared to CH_4 liquid. This indicate that different type of liquid molecules will generate different heat transport at the S-L interfaces although both molecules of CH_4 and C_4H_{10} liquids consisted of the same atoms which is hydrogen and carbon.

Table 2
Thermal boundary resistance (TBR) in x, y and z-component for CH_4 and C_4H_{10}

Crystal plane	CH_4 (Methane) TBR (m^2K/W X 10^{-6})				C_4H_{10} (Butane) TBR (m^2K/W X 10^{-6})			
	Total	x	y	z	Total	x	y	z
100	0.1215	1.9980	1.7600	0.1396	0.1222	1.8260	1.9590	0.1403
110	0.0907	1.8780	0.3898	0.1262	0.1131	1.8090	0.6401	0.1486
111	0.1031	2.569	2.029	0.1134	0.1112	2.6330	1.9940	0.1232

4. Conclusions

The characteristics of heat transport at the S-L interfaces was investigated using molecular dynamics simulations. It is found that the temperature jump existed at the S-L interfaces. This different temperature jump is observed for different surface structure of face-centered cubic (FCC) lattices and different types of liquid molecules. The thermal boundary resistance (TBR) is correlated with the temperature jump where large temperature jump exhibits a large TBR. It is also observed that there is variation of temperature jump and TBR depending on the different types of liquid molecules. Lastly, from the results, it is suggested that the characteristics of heat transport across the S-L interfaces is significantly influenced by the surface structure of the FCC lattice and the types of liquid molecules.

Acknowledgement

References
[1] Michalczewski, Remigiusz, Witold Piekoszewski, Marian Szczerek, and Waldemar Tuszynski. "The lubricant-coating interaction in rolling and sliding contacts." *Tribology International* 42, no. 4 (2009): 554-560.
[2] Kalin, M., E. Roman, L. Ožbolt, and J. Vižintin. "Metal-doped (Ti, WC) diamond-like-carbon coatings: reactions with extreme-pressure oil additives under tribological and static conditions." *Thin Solid Films* 518, no. 15 (2010): 4336-4344.
[3] Abdullah, M. I. H. C., Mohd Fadzli Bin Abdollah, Hilmi Amiruddin, Nur Rashid Mat Nuri, Noreffendy Tamaldin,

Masjuki Hassan, and S. A. Rafeq. "Effect of hBN/Al2O3 nanoparticles on engine oil properties." *Energy Education Science and Technology Part A: Energy Science and Research* 32, no. 5 (2014): 3261-3268.

[4] Zin, Mohd Rody Bin Mohamad, Kiichi Okuno, Keiji Sasaki, Naruhiko Inayoshi, Noritsugu Umehara, Hiroyuki Kousaka, and Shingo Kawara. "Depth Profile of Oxygen of Diamond-Like Carbon Sliding under Pressurized Hot Water." *Tribology Online* 12, no. 1 (2017): 8-17.

[5] F.A. Munir, M. Mikami, M.Z. Hassan, M.A. Salim. "Flame stabilization in multiple inlet channel meso-scale tube combustors with wire mesh." *J. Adv. Veh. Syst.* 1 (2017): 20–27.

[6] Aizawa, T., A. Mitsuo, S. Yamamoto, T. Sumitomo, and S. Muraishi. "Self-lubrication mechanism via the in situ formed lubricious oxide tribofilm." *Wear* 259, no. 1-6 (2005): 708-718.

[7] Wang, H. M., Y. L. Yu, and S. Q. Li. "Microstructure and tribological properties of laser clad CaF2/Al2O3 self-lubrication wear-resistant ceramic matrix composite coatings." *Scripta Materialia* 47, no. 1 (2002): 57-61.

[8] Podgornik, B., M. Sedlaček, and Dj Mandrino. "Performance of CrN coatings under boundary lubrication." *Tribology International* 96 (2016): 247-257.

[9] Neto, Chiara, Drew R. Evans, Elmar Bonaccurso, Hans-Jürgen Butt, and Vincent SJ Craig. "Boundary slip in Newtonian liquids: a review of experimental studies." *Reports on Progress in Physics* 68, no. 12 (2005): 2859.

[10] Thompson, Peter A., and Sandra M. Troian. "A general boundary condition for liquid flow at solid surfaces." *Nature* 389, no. 6649 (1997): 360.

[11] Ohara, Taku. "Intermolecular energy transfer in liquid water and its contribution to heat conduction: A molecular dynamics study." *The Journal of chemical physics* 111, no. 14 (1999): 6492-6500.

[12] Ohara, Taku. "Contribution of intermolecular energy transfer to heat conduction in a simple liquid." *The Journal of chemical physics* 111, no. 21 (1999): 9667-9672.

[13] Ohara, Taku, and Daichi Torii. "Molecular dynamics study of thermal phenomena in an ultrathin liquid film sheared between solid surfaces: The influence of the crystal plane on energy and momentum transfer at solid-liquid interfaces." *The Journal of chemical physics* 122, no. 21 (2005): 214717.

[14] Khare, Rajesh, Pawel Keblinski, and Arun Yethiraj. "Molecular dynamics simulations of heat and momentum transfer at a solid–fluid interface: relationship between thermal and velocity slip." *International journal of heat and mass transfer* 49, no. 19-20 (2006): 3401-3407.

[15] Ohara, Taku, and Daichi Torii. "Molecular thermal phenomena in an ultrathin lubrication liquid film of linear molecules between solid surfaces." *Microscale Thermophysical Engineering* 9, no. 3 (2005): 265-279.

[16] Torii, Daichi, and Taku Ohara. "Molecular dynamics study on ultrathin liquid water film sheared between platinum solid walls: Liquid structure and energy and momentum transfer." *The Journal of chemical physics* 126, no. 15 (2007): 154706.

[17] Sun, Jie, Wen Wang, and Hua Sheng Wang. "Dependence between velocity slip and temperature jump in shear flows." *The Journal of chemical physics* 138, no. 23 (2013): 234703.

[18] Ameur, Djilali, and Guillaume Galliéro. "Slippage of binary fluid mixtures in a nanopore." *Microfluidics and nanofluidics* 15, no. 2 (2013): 183-189.

[19] Pahlavan, Amir Alizadeh, and Jonathan B. Freund. "Effect of solid properties on slip at a fluid-solid interface." *Physical Review E* 83, no. 2 (2011): 021602.

[20] Priezjev, Nikolai V., and Sandra M. Troian. "Molecular origin and dynamic behavior of slip in sheared polymer films." *Physical review letters* 92, no. 1 (2004): 018302.

[21] Mohamad Shukri Zakaria, Farzad Ismail, Masaaki Tamagawa, Ahmad Fazli Abdul Azi, Surjatin Wiriadidjaya, Adi Azrif Basri, Kamarul Arifin Ahmad, "Computational Fluid Dynamics Study of Blood Flow in Aorta using OpenFOAM." *Journal of Advanced Research in Fluid Mechanics and Thermal Sciences* 43 (2018): 81–89.

[22] Priezjev, Nikolai V. "Effect of surface roughness on rate-dependent slip in simple fluids." *The Journal of chemical physics* 127, no. 14 (2007): 144708.

[23] Soong, C. Y., T. H. Yen, and P. Y. Tzeng. "Molecular dynamics simulation of nanochannel flows with effects of wall lattice-fluid interactions." *Physical Review E* 76, no. 3 (2007): 036303.

[24] Nath, Shyamal K., and Rajesh Khare. "New forcefield parameters for branched hydrocarbons." *The Journal of Chemical Physics* 115, no. 23 (2001): 10837-10844.

[25] S. Nath, Shyamal K., Fernando A. Escobedo, and Juan J. de Pablo. "On the simulation of vapor–liquid equilibria for alkanes." *The Journal of Chemical Physics* 108, no. 23 (1998): 9905-9911.

[26] Bin Saleman, Abdul Rafeq, Hari Krishna Chilukoti, Gota Kikugawa, Masahiko Shibahara, and Taku Ohara. "A molecular dynamics study on the thermal transport properties and the structure of the solid–liquid interfaces between face centered cubic (FCC) crystal planes of gold in contact with linear alkane liquids." *International Journal of Heat and Mass Transfer* 105 (2017): 168-179.

[27] bin Saleman, Abdul Rafeq, Hari Krishna Chilukoti, Gota Kikugawa, Masahiko Shibahara, and Taku Ohara. "A molecular dynamics study on the thermal energy transfer and momentum transfer at the solid-liquid interfaces

between gold and sheared liquid alkanes." *International Journal of Thermal Sciences* 120 (2017): 273-288.

[28] Chilukoti, Hari Krishna, Gota Kikugawa, and Taku Ohara. "Structure and transport properties of liquid alkanes in the vicinity of α-quartz surfaces." *International Journal of Heat and Mass Transfer* 79 (2014): 846-857.

[29] Martin, Marcus G., and J. Ilja Siepmann. "Transferable potentials for phase equilibria. 1. United-atom description of n-alkanes." *The Journal of Physical Chemistry B* 102, no. 14 (1998): 2569-2577.

[30] Kikugawa, Gota, Taku Ohara, Toru Kawaguchi, Eiichi Torigoe, Yasumasa Hagiwara, and Yoichiro Matsumoto. "A molecular dynamics study on heat transfer characteristics at the interfaces of alkanethiolate self-assembled monolayer and organic solvent." *The Journal of chemical physics* 130, no. 7 (2009): 074706.

[31] Boccara, Nino. "The Morse Potential." *Essentials of Mathematica: With Applications to Mathematics and Physics*(2007): 445-448.

[32] Rappé, Anthony K., Carla J. Casewit, K. S. Colwell, W. A. Goddard Iii, and W. M. Skiff. "UFF, a full periodic table force field for molecular mechanics and molecular dynamics simulations." *Journal of the American chemical society* 114, no. 25 (1992): 10024-10035.

[33] Vo, Truong Quoc, Murat Barisik, and BoHung Kim. "Atomic density effects on temperature characteristics and thermal transport at grain boundaries through a proper bin size selection." *The Journal of chemical physics* 144, no. 19 (2016): 194707.